STRUCTURE AND CHEMISTRY OF A SUPERNOVA ORTHOPYROXENE GRAIN IN THE CO CHONDRITE DOMINION RANGE 08006. L. B. Seifert[1], P. Haenecour[1], T. Ramprasad[1,2], and T. J. Zega[1,2]. Lunar and Planetary Laboratory, University of Arizona, 1629 E University Blvd. Tucson, AZ, 85721-0092, lseifert@lpl.arizona.edu. [2] Materials Science and Engineering, University of Arizona.

Introduction: In the concluding evolutionary stages of its life, a massive star exhausts its nuclear fuel and can experience a collapse of its stellar core. This collapse can cause a rebound shockwave to propagate through the evolved stellar structure, triggering a violent explosion of material radially away from its center in the form of a supernova. Solids can condense in this ejected material and transport through the interstellar medium (ISM). Some such materials have been preserved in primitive meteorites [e.g. 1].

The crystal chemistry, isotopic composition, and atomic structure of these materials can provide ground-truth information on the origins of their parent stars. Several studies to analyze and understand the structure and chemistry of silicate and oxide grains derived from supernovae were reported [2-8]. These studies reveal grains with diverse structures, compositions, sizes and morphologies indicative of the varied histories that they have experienced in the ejecta of their progenitor stars. Here we report results on a supernova silicate grain identified in the Dominion Range (DOM) 08006 CO3.0 chondrite. This work is part of a broader effort to understand the detailed crystal chemistry and structure of presolar grains and what they tell us about their stellar origins, transport through the ISM, and their survival and preservation during solar-system formation.

Sample and Methods: Isotopically anomalous regions were identified in a petrographic thin section of DOM 08006 via NanoSIMS raster-ion-imaging of O and C isotopes at Washington University in St. Louis [9]. Major-element compositions for the anomalous regions were obtained by Auger spectroscopy [9]. One anomalous region, DOM-39, was chosen for detailed structural and chemical analysis using transmission electron microscopy (TEM).

Well-established focused ion-beam scanning-electron microscopy (FIB-SEM) techniques [10] were used to prepare an electron-transparent cross section of DOM-39 with the Thermo Fischer (formerly FEI) Helios G^3 FIB-SEM located at the Lunar and Planetary Laboratory (LPL). The FIB section was then analyzed with the 200 keV aberration-corrected Hitachi HF5000 S/TEM at LPL. The HF5000 is equipped with secondary electron (SE) detectors, scanning TEM (STEM)-based bright-field (BF) and dark-field (DF) imaging detectors, as well as an Oxford Instruments X-Max^N

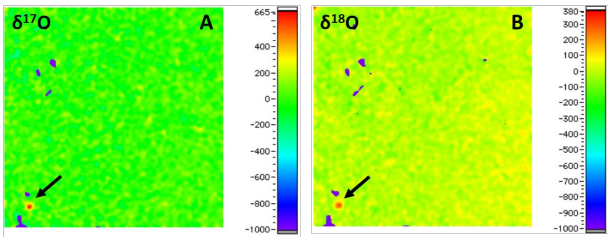

Figure 1: NanoSIMS $\delta^{17}O$ (A) and $\delta^{18}O$ (B) images with arrow indicating circular anomalous region and enrichments in ^{17}O and ^{18}O.

100 TLE EDS system with dual 100 mm^2 windowless silicon-drift detectors (solid angle of 2 sr).

Results: NanoSIMS analysis of the local region of DOM-39 reveals enrichment in both ^{17}O and ^{18}O relative to solar system values, with $^{17}O/^{16}O = 6.4E^{-4} \pm 3.0E^{-5}$ and $^{18}O/^{16}O = 2.64E^{-3} \pm 7.0E^{-6}$ [9]. These isotopic compositions place DOM-39 in the Group 4 field of circumstellar grains as defined by [11]. NanoSIMS raster-ion-imaging reveals a round O-anomaly and measures roughly 275 × 275 nm (Fig. 1) as confirmed by TEM data.

S/TEM imaging of DOM-39 shows a well-defined grain with a bright footprint-shaped feature in the upper left portion of the grain (Fig. 2). The footprint measures between 40 and 50 nm in width and 130 nm in length and has a rim surrounding it. STEM-EDS mapping of the entire FIB section reveals that the matrix surrounding DOM-39 contains O, Si, Mg, Fe, Ca, and localized S and Ni. DOM-39 contains spatial correlations among O, Si, Mg, and Fe in the grain and the footprint region contains spatial correlations among Fe, Ni, and S (Fig. 2).

Selected-area electron-diffraction (SAED) patterns were collected across the grain and footprint region. DOM-39 is a crystalline, stoichiometric orthopyroxene grain and the footprint region is consistent with a non-stoichiometric pyrrhotite.

Discussion: The structure and chemistry of presolar grains record thermodynamic properties, which can provide information on stellar origins. Equilibrium thermodynamic models can provide first-order constraints on the origins of circumstellar grains [e.g. 12]. There are models of dust condensation in supernovae available in the literature for both equilibrium and kinetic processes. Fedkin et al. [13] used model compositions of thin layers of ejecta computed by [14] in

order to obtain the chemical compositions of minerals condensed via equilibrium processes in 15-, 20- and 25- $M_\odot$ supernovae. The condensation sequences and formation temperatures are similar for all three masses [13]. In comparison, Nozawa et al. [15] and Todini and Ferrera [16] used nucleation theory to model kinetic processes supernovae ejecta.

Comparison of the grain data with these equilibrium and kinetic condensation models can help place constraints on the progenitor supernova of DOM-39. In comparison to equilibrium thermodynamic model predications by [13], the $^{16}O/^{18}O$ ratio of DOM-39 is most consistent with a 15 $M_\odot$ supernova. The crystalline orthopyroxene grain could have condensed via equilibrium processes in a 15 to 25 $M_\odot$ supernova between 1100 and 1548K [13]. The kinetic models of [15] and [16] do not explicitly discuss orthopyroxene, but note that Mg-rich pyroxenes are expected to condense between 1400 and 1500 K[15] and around 1100 K [16]. Although the kinetic models do not discuss orthopyroxene, the condensation temperatures for Mg-rich pyroxenes are within the range suggested for orthopyroxene via equilibrium processes. Therefore, it is possible DOM-39 could have condensed via equilibrium.

We hypothesize that the orthopyroxene provided a nucleation site for the growth of pyrrhotite. Iron sulfide is more volatile than pyroxene and so is predicted to condense at lower temperatures, *e.g.,* 704 K for troilite vs. 1316 K for a Mg-rich pyroxene at a total pressure of 10^{-4} bar [e.g. 12]. It is therefore plausible that as temperature cooled in the progenitor supernova ejecta of DOM-39, that orthopyroxene condensed first and provided a nucleation site for pyrrhotite condensation. Alternatively, the pyrrhotite could have condensed onto DOM-39 in the solar-protoplanetary disk. A possible test of this hypothesis could be provided by follow up isotopic measurements with NanoSIMS.

We also note that the pyrrhotite region has a rim around it, suggesting secondary processing occurred. It is unclear whether this processing took place in the ISM or in the solar nebula. Nonetheless, it appears that the supernova orthopyroxene grain was not affected by such processing.

Acknowledgments: We gratefully acknowledge the late Professor Christine Floss for her contributions to the identification of DOM-39 through NASA grants NNX14AG25G and NNX12AN77H. The research completed here was supported by NASA grants NNX15AJ22G and 80NSSC19K0509. We also acknowledge NASA grants NNX12AL47G, NNX15AJ22G, 80NSSC19K0509, and NSF grant 1531243 for funding instrumentation in the Kuiper Materials Imaging and Characterization Facility at LPL.

References: [1] Zinner E. (2014) Elsevier Ltd, 181. [2] Messenger, S., et al., (2005), Science, 309, 737. [3] Floss, C. et al., (2006), GCA, 70, 2371. [4] Zega, T., et al., (2011), ApJ, 730, 83. [5] Nguyen, A. et al., (2011), 74th MetSoc, #5449 (abstr.). [6] Nguyen, A. et al., (2016), ApJ, 818, 51. [7] Takigawa, A., et al., (2014), LPSC XLV, #1465 (abstr.). [8] Seifert et al., (2019), LPSC L, #2585 (abstr.). [9] Haenecour P. et al. (2018) *GCA* 221: 379-405. [10] Zega T. et al., (2007) *MAPS* 42: 1373-1386. [11] Nittler L. et al. (1997) ApJ, 483, 475-495. [12] Lodders, K., (2003), ApJ, 591, 1220. [13] Fedkin, A., et al. (2010) GCA, 74, 3658. [14] Rauscher, T., et al., (2002), ApJ, 576, 323. [15] Nozawa, T., et al., (2003), ApJ, 598, 785. [16] Todini and Ferrera (2001), MNRAS 325, 726.

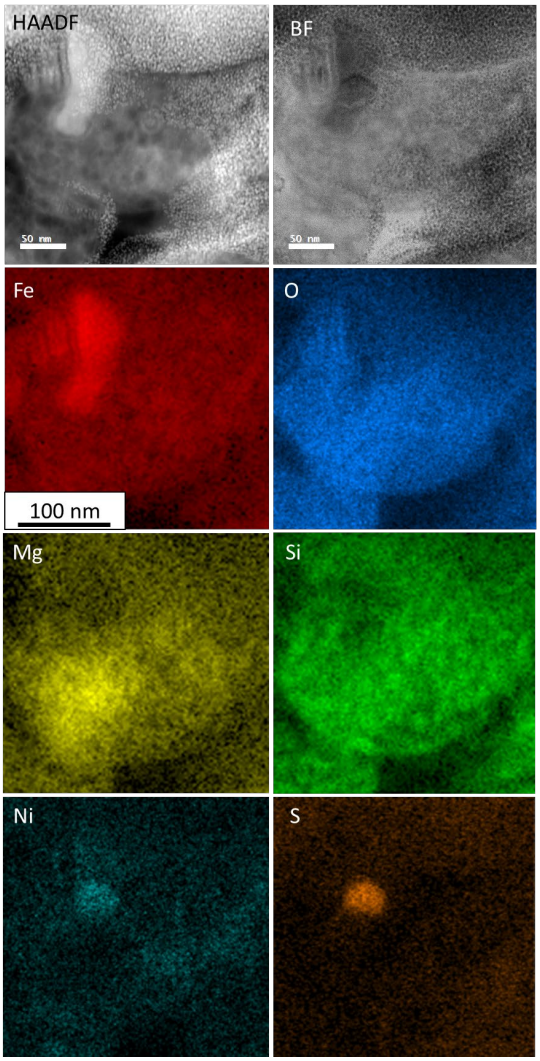

Figure 2: EDS maps of DOM-39 with high-angle annular dark-field (HAADF) and bright field (BF) images for comparison.